Nonlocal Dispersive Model For Wave Propagation In Heterogeneous Media. Part 1: One-Dimensional Case

Jacob Fish, Wen Chen and Gakuji Nagai

Departments of Civil, Mechanical and Aerospace Engineering

Rensselaer Polytechnic Institute, Troy, NY 12180, USA

Abstract: Nonlocal dispersive model for wave propagation in heterogeneous media is derived from the higher-order mathematical homogenization theory with multiple spatial and temporal scales. In addition to the usual space-time coordinates, a fast spatial scale and a slow temporal scale are introduced to account for rapid spatial fluctuations of material properties as well as to capture the long-term behavior of the homogenized solution. By combining various order homogenized equations of motion the slow time dependence is eliminated giving rise to the fourth-order differential equation, also known as a "bad" Boussinesq problem. Regularization procedures are then introduced to construct so called "good" Bouinesq problem, where the need for C^1 continuity is eliminated. Numerical examples are presented to validate the present formulation.

1. Introduction

The use of multiple-scale expansions as a systematic tool of averaging can be traced to Sanchez-Palencia [1], Benssousan, Lions and Papanicoulau [2], and Bakhvalov and Panasenko [3]. The role of higher order terms in the asymptotic expansion has been investigated in statics by Gambin and Kroner [4], and Boutin [5]. In elastodynamics, Boutin and Auriault [6] demonstrated that the terms of a higher order successively introduce effects of polarization, dispersion and attenuation. In [6][7] a single-frequency time dependence was assumed prior to the homogenization process.

A general setting for the initial-boundary value problem in heterogeneous media has been presented by the first two authors in [8][9], where it has been demonstrated that while the high-order homogenization is capable of capturing dispersion effects for relatively short observation time window, it introduces secular terms which grow unbounded with time. The problem of secularity has been successfully resolved with the introduction of slow temporal scales to capture the long-term behavior of the homogenized solution [8][9].

The primary objective of the current manuscript is to develop a nonlocal approach independent of slow time scale considered in [8][9]. We show that by adding various order homogenized equations of motion resulting from the higher mathematical homogenization in space and time [8][9] the slow time scale dependence can be eliminated. The resulting equation, also known as "bad" Boussinesq equation, contains a fourth-order spatial derivative term and has no solution for high frequency load excitations. This problem is alleviated by approximating the fourth-order spatial derivative with a mixed spatial-temporal derivative and thus yielding the so called "good" Boussinesq equation, which is well-posed. It contains only the second-order spatial-temporal derivatives and thus eliminating the need for C^1 continuous elements. The weak formulation and the finite element approximation leads to the semi-discrete equations of motion, which are then integrated by using standard time integration schemes.

The outline of the manuscript is as follows. Problem description and high-order homogenization with multiple space-time scales are reviewed in Section 2 and 3, respectively. Nonlocal models are derived in Section 4. Finite element procedures for solving the nonlocal equations of motion are formulated in Section 5. Section 6 gives numerical examples.

2. Problem Description

We consider wave propagation normal to the layers of an array of periodic elastic bilaminates with l as a characteristic length (see Figure 1).

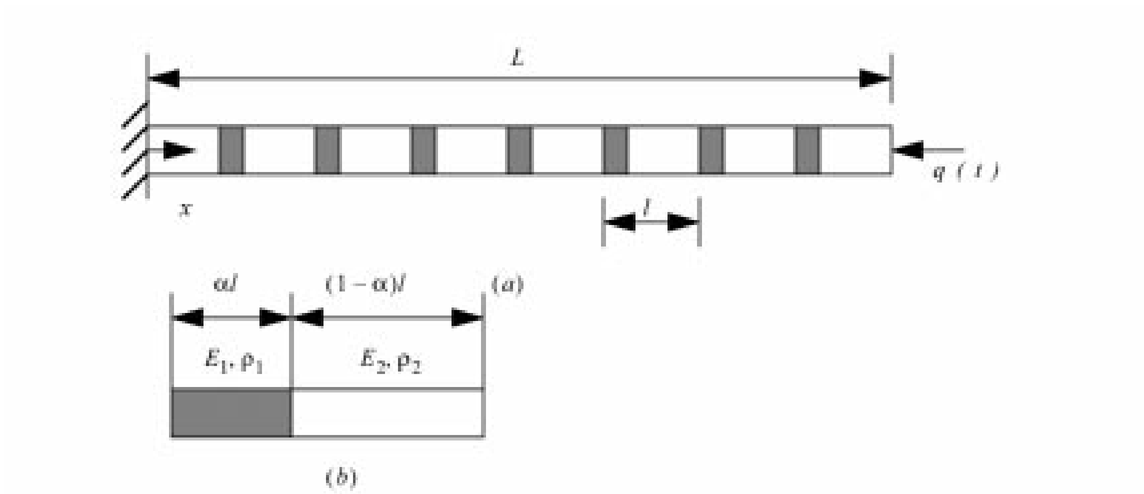

Figure 1: A bilaminate with periodic microstructure

The governing equation for the elastodynamics problem is given by

$$\rho(x/\varepsilon)u_{;tt} - \{E(x/\varepsilon)u_{;x}\}_{;x} = 0 \tag{1}$$

with appropriate boundary conditions on the domain boundary ∂L

$$u(0, t) = 0, \quad u_{;x}(L, t) = \frac{q(t)}{E(L)A} \tag{2}$$

and initial conditions

$$u(x, 0) = f(x), \quad u_{;t}(x, 0) = g(x) \tag{3}$$

where $u(x, t)$ represents the displacement field; $\rho(x/\varepsilon)$, $E(x/\varepsilon)$, A and $q(t)$ the mass density, elastic modulus, cross-sectional area and external load, respectively; $(\ )_{;x}$ and

$(\ )_{;t}$ denote differentiation with respect to space and time, respectively; $0 < \varepsilon \ll 1$ in (1) denotes the rapid spatial variation of material properties. The goal is to establish an effective homogeneous model in which local fluctuations introduced by material heterogeneity do not appear explicitly and the response of a heterogeneous medium can be approximated by the response of the effective homogeneous medium. This is facilitated by the method of multiple scale asymptotic expansion in space and time.

3. Asymptotic Analysis with Multiple Space-Time Scales

Under the premise that the macroscopic domain $L = \lambda/(2\pi)$ is much larger than the unit cell domain l, i.e. $l/L = (\omega l)/c = kl \ll 1$, it is convenient to introduce a microscopic spatial length variable y [6][13] such that

$$y = x/\varepsilon \tag{4}$$

where λ, ω, k and c are the macroscopic wavelength, the circular frequency, the wave number and the phase velocity of the macroscopic wave, respectively. In addition to the fast spatial variable, we introduce multiple time scales [8][9]

$$\eta = t, \quad \tau = \varepsilon^2 t \tag{5}$$

where η denotes the usual time scale and τ is a slow time scale. Since the response quantities u and σ depend on x, y, η and τ, a multiple-scale asymptotic expansion is employed to approximate the displacement and stress fields

$$u(x, y, \eta, \tau) = \sum_{i=0}^{n} \varepsilon^i u_i(x, y, \eta, \tau), \quad \sigma(x, y, \eta, \tau) = \sum_{i=-1}^{n} \varepsilon^i \sigma_i(x, y, \eta, \tau) \tag{6}$$

Asymptotic analysis consists of inserting asymptotic expansions (6) into the governing equation (1), identifying the terms with equal power of ε, and finally, solving the resulting problems.

Following the aforementioned procedure and expressing the spatial and temporal derivatives using the chain rule

$$u_{;x} = u_{,x} + \varepsilon^{-1} u_{,y}, \quad u_{;t} = u_{,\eta} + \varepsilon^2 u_{,\tau} \tag{7}$$

we obtain a series of equations in ascending power of ε starting at ε^{-2}. We successively equate the factors of each of these powers to zero.

3.1 $O(1)$ homogenization

At $O(\varepsilon^{-2})$, we have

$$\{E(y)u_{0,y}\}_{,y} = 0 \tag{8}$$

The general solution to the above equation is

$$u_0 = a_1(x, \eta, \tau)\int_{y_0}^{y_0+y} \frac{1}{E(\zeta)}d\zeta + a_2(x, \eta, \tau) \tag{9}$$

where $a_1(x, \eta, \tau)$ and $a_2(x, \eta, \tau)$ are functions of macro coordinates. To ensure periodicity of u_0 over the unit cell domain $\hat{l} = l/\varepsilon$ ($\hat{(\ )}$ denotes quantities in the stretched coordinate system *y*), a_1 must vanish, implying that the leading-order displacement depends only on the macroscale

$$u_0 = u_0(x, \eta, \tau) \tag{10}$$

At $O(\varepsilon^{-1})$, the perturbation equation is

$$\{E(y)(u_{0,x} + u_{1,y})\}_{,y} = 0 \tag{11}$$

Due to linearity of the above equation, the general solution to u_1 is

$$u_1(x, y, \eta, \tau) = U_1(x, \eta, \tau) + H(y)u_{0,x} \tag{12}$$

Substituting (12) into (11) yields

$$\{E(y)(1 + H_{,y})\}_{,y} = 0 \tag{13}$$

For a $\hat{l}$ -periodic function $G(x, y, \eta, \tau)$, we define an averaging operator

$$\langle G\rangle = \frac{1}{|\hat{l}|}\int_{\hat{l}} G(x, y, \eta, \tau)dy \tag{14}$$

The boundary conditions for the unit cell problem described by (13) are

(a) Periodicity: $u_1(y = 0) = u_1(y = \hat{l})$, $\sigma_0(y = 0) = \sigma_0(y = \hat{l})$

(b) Continuity: $[u_1(y = \alpha\hat{l})] = 0$, $[\sigma_0(y = \alpha\hat{l})] = 0$

(c) Normalization: $\langle u_1(x, y, \eta, \tau)\rangle = U_1(x, \eta, \tau) \Rightarrow \langle H(y)\rangle = 0$ (15)

where $0 \le \alpha \le 1$ is the volume fraction of the unit cell; $[\ \ ]$ is the jump operator and

$$\sigma_i = E(y)(u_{i,x} + u_{i+1,y}), \qquad i = 0, 1, \ldots, n \tag{16}$$

Equation (13) together with the boundary conditions (15) define the unit cell boundary value problem from which $H(y)$ can be uniquely determined:

$$H_1(y) = \frac{(1-\alpha)(E_2 - E_1)}{(1-\alpha)E_1 + \alpha E_2}\left\{y - \frac{\alpha\hat{l}}{2}\right\}, \quad H_2(y) = \frac{\alpha(E_1 - E_2)}{(1-\alpha)E_1 + \alpha E_2}\left\{y - \frac{(1+\alpha)\hat{l}}{2}\right\} \tag{17}$$

At $O(1)$, the perturbation equation is

$$\rho(y)u_{0,\eta\eta} - \{E(y)(u_{0,x} + u_{1,y})\}_{,x} - \{E(y)(u_{1,x} + u_{2,y})\}_{,y} = 0 \tag{18}$$

Applying the averaging operator defined in (14) to the above equation and accounting for the periodicity of σ_1, yields the macroscopic equation of motion at $O(1)$:

$$\rho_0 u_{0,\eta\eta} - E_0 u_{0,xx} = 0 \tag{19}$$

where

$$\rho_0 = \langle\rho\rangle = \alpha\rho_1 + (1-\alpha)\rho_2, \quad E_0 = \langle E(y)(1 + H_{,y})\rangle = \frac{E_1 E_2}{(1-\alpha)E_1 + \alpha E_2}. \tag{20}$$

3.2 $O(\varepsilon)$ homogenization

u_2 is determined from the $O(1)$ perturbation equation (18). Substituting (12) and (19) into (18) gives

$$\{E(y)(u_{2,y} + U_{1,x} + Hu_{0,xx})\}_{,y} = \{(\theta(y) - 1)E_0\}u_{0,xx} \tag{21}$$

where

$$\theta(y) = \rho(y)/\rho_0 \tag{22}$$

Linearity suggests that u_2 may be sought in the form

$$u_2(x, y, \eta, \tau) = U_2(x, \eta, \tau) + H(y)U_{1,x} + P(y)u_{0,xx} \tag{23}$$

Substituting the above expression into (21) yields

$$\{E(y)(H + P_{,y})\}_{,y} = (\theta(y) - 1)E_0 \tag{24}$$

The boundary conditions for the above equation are: periodicity and continuity of u_2 and σ_1 as well as the normalization condition $\langle P(y)\rangle = 0$. $P(y)$ can be uniquely determined by solving the unit cell boundary value problem defined by (24). For details we refer to [8]. Once $P(y)$ is found, we can calculate

$$\langle \rho H \rangle = 0, \qquad \langle E(H + P_{,y}) \rangle = 0 \tag{25}$$

Next we consider the $O(\varepsilon)$ equilibrium equation

$$\rho(y) u_{1,\eta\eta} - \{E(y)(u_{1,x} + u_{2,y})\}_{,x} - \{E(y)(u_{2,x} + u_{3,y})\}_{,y} = 0 \tag{26}$$

Applying the averaging operator to (26) and exploiting periodicity of σ_2, we derive the macroscopic equation of motion at $O(\varepsilon)$

$$\rho_0 U_{1,\eta\eta} - E_0 U_{1,xx} = 0 \tag{27}$$

3.3 $O(\varepsilon^2)$ homogenization

u_3 is determined from $O(\varepsilon)$ perturbation equation (26). Substituting (12), (23) into (26) and making use of the macroscopic equations of motion (19) and (27), we have

$$\{E(y)(u_{3,y} + U_{2,x} + HU_{1,xx} + Pu_{0,xxx})\}_{,y} =$$

$$\{\theta(y)E_0 H - E(y)(H + P_{,y})\}u_{0,xxx} + \{(\theta(y) - 1)E_0\}U_{1,xx} \tag{28}$$

Owing to linearity of (28), the general solution to u_3 is as follows

$$u_3(x, y, \eta, \tau) = U_3(x, \eta, \tau) + H(y)U_{2,x} + P(y)U_{1,xx} + Q(y)u_{0,xxx} \tag{29}$$

Substituting (29) into (28) gives

$$\{E(y)(P + Q_{,y})\}_{,y} = \theta(y)E_0 H - E(y)(H + P_{,y}) \tag{30}$$

The above equation, together with periodicity and continuity of u_3 and σ_2 as well as the normalization condition $\langle Q(y) \rangle = 0$, fully determine $Q(y)$.

Consider the equilibrium equation of $O(\varepsilon^2)$:

$$\rho(y)(u_{2,\eta\eta} + 2u_{0,\eta\tau}) - \{E(y)(u_{2,x} + u_{3,y})\}_{,x} - \{E(y)(u_{3,x} + u_{4,y})\}_{,y} = 0 \tag{31}$$

Applying the averaging operator to (31) and taking into account periodicity of σ_3 yields

$$\langle \rho u_{2,\eta\eta} \rangle + 2\rho_0 u_{0,\eta\tau} - \{\langle E(y)(u_{2,x} + u_{3,y}) \rangle\}_{,x} = 0 \tag{32}$$

Substituting (23) and (29) into (32) yields

$$\rho_0 U_{2,\eta\eta} - E_0 U_{2,xx} = \{\langle E(y)(P + Q_{,y})\rangle - \langle \rho P \rangle E_0 / \rho_0\} u_{0,xxxx} - 2\rho_0 u_{0,\eta\tau} \tag{33}$$

Inserting the expressions for $P(y)$ and $Q(y)$ into (33) and averaging over the unit cell domain yields the macroscopic equation of motion at the second order:

$$\rho_0 U_{2,\eta\eta} - E_0 U_{2,xx} = \frac{1}{\varepsilon^2} E_d u_{0,xxxx} - 2\rho_0 u_{0,\eta\tau} \tag{34}$$

where

$$E_d = \frac{[\alpha(1-\alpha)]^2 (E_1\rho_1 - E_2\rho_2)^2 E_0 l^2}{12\rho_0^2 [(1-\alpha)E_1 + \alpha E_2]^2} \tag{35}$$

E_d characterizes the effect of the microstructure on the macroscopic behavior. It is proportional to the square of the dimension of the unit cell l. Note that for the homogeneous material, $\alpha = 0$ or $\alpha = 1$, and in the case of identical impedance of two material constituents $r = z_2/z_1 = 1$ ($z = \sqrt{E\rho}$), E_d vanishes.

Remark 1: It can be easily shown that in the case of equal mass density, $\rho_1 = \rho_2$, the following identity holds:

$$\hat{E}_d = \langle E(y)(P + Q_{,y})\rangle = \langle H(y)H(y)\rangle E_0 \tag{36}$$

where $\hat{E}_d$

$$E_d = \varepsilon^2 \hat{E}_d \tag{37}$$

The significance of (36) is that $\hat{E}_d$ can be evaluated by averaging over the leading-order unit cell solution without consideration of the higher-order boundary value problem in the unit cell. This feature will greatly simplify numerical computations in multi-dimensional case [20].

4. Nonlocal models

The macroscopic equations of motion are stated in (19), (27) and (34). The initial and boundary conditions for the above equations of motion are prescribed as

$$\text{ICs:}\quad u_0(x,0,0) = f(x)\,,\quad u_{0;t}(x,0,0) = g(x)$$

$$U_i(x,0,0) = 0\,,\quad U_{i;t}(x,0,0) = 0 \quad (i = 1, 2) \tag{38}$$

BCs: $u_0(0, \eta, \tau) = 0, \quad u_{0,x}(L, \eta, \tau) = \frac{q(t)}{E_0 A}$

$$U_i(0, \eta, \tau) = 0, \quad U_{i,x}(L, \eta, \tau) = 0 \quad (i = 1, 2) \tag{39}$$

The above initial-boundary value problem is well-posed. From the equation of motion (27) and the initial and boundary conditions (38) and (39), we can readily deduce that $U_1(x, \eta, \tau) \equiv 0$.

In [9] we have shown that the dispersive solution can be obtained by solving the leading-order macroscopic equation of motion (19) subjected to the secularity constraint

$$\frac{E_d}{\varepsilon^2} u_{0,xxxx} - 2\rho_0 u_{0,\eta\tau} = 0. \tag{40}$$

The above formulation necessitates simultaneous solution of two sets of partial differential equations with two temporal coordinates. In this section we will derive an alternative formulation in attempt to eliminate the dependence on the slow time coordinate.

We start by defining the mean displacement $U(x, t)$ as

$$U(x, t) = \langle u(x, y, \eta, \tau) \rangle = u_0(x, \eta, \tau) + \varepsilon U_1(x, \eta, \tau) + \varepsilon^2 U_2(x, \eta, \tau) + \dots \tag{41}$$

Adding (19), (27) and (34), and neglecting terms of order $O(\varepsilon^3)$ and higher, we obtain an equation of motion for the mean displacement

$$\rho_0 \ddot{U} - E_0 U_{,xx} - E_d U_{,xxxx} = 0 \tag{42}$$

where $\ddot{U} = U_{;tt}$ denotes the second full time derivative of the mean displacement. Equation (42) is fourth-order in space. It necessitates four boundary conditions to define a well-posed boundary value problem. However, for the problem under consideration, there are only two physically meaningful boundary conditions for the mean displacement. Mathematically similar equation to (42) arises in fluid dynamics of shallow water theory and crystal-lattice theory, and is often known as a “bad” Boussinesq equation (cf. [16][17]).

To study the characteristics of the so called “bad” Boussinesq equation (42), we consider a model problem with an initial disturbance in the displacement field at one end and load free at the other. We compliment two artificial boundary conditions

$$U_{,xx}(0, t) = 0, \quad U_{,xxx}(L, t) = 0 \tag{43}$$

The solution to the above initial-boundary value problem can be obtained in close form:

$$U(x, t) = \sum_{n=1}^{\infty} B_n \sin\frac{p_n x}{L} \cos\left\{\left[\sqrt{1 - \frac{E_d}{E_0 L^2}(p_n)^2}\right] p_n ct/L\right\} \tag{44}$$

where

$$c = \sqrt{E_0/\rho_0}, \quad p_n = (2n-1)\frac{\pi}{2}, \tag{45}$$

$$B_n = \frac{2}{L}\int_0^L f(x) \sin\frac{p_n x}{L} dx \quad , \quad (n = 1, 2, 3, \ldots) \tag{46}$$

Solution (44) is considered “bad” since for higher order terms in the Fourier series the value in the square root is negative making the solution meaningless.

In comparison, the exact solution of macroscopic equation of motion (34) subjected to secularity constraint (40) is given as [9]:

$$u_d(x, t) = \sum_{n=1}^{\infty} B_n \sin\frac{p_n x}{L} \cos\left\{\left(1 - \frac{E_d}{2E_0 L^2}(p_n)^2\right) p_n ct/L\right\} \tag{47}$$

The Taylor’s series expansion of square root term in (44) is given as:

$$\sqrt{1 - \frac{E_d}{E_0 L^2}(p_n)^2} = 1 + \left(-\frac{E_d}{2E_0 L^2}(p_n)^2\right) - \frac{1}{8}\left(\frac{E_d}{E_0 L^2}(p_n)^2\right)^2 - \ldots \tag{48}$$

Note that $\frac{E_d}{E_0 L^2} = O\left(\frac{l^2}{L^2}\right) = O(\varepsilon^2)$ and thus if $p_n = O(1/\varepsilon^{\beta})$ with $\beta < 1$ then the higher order terms in (48) can be neglected and the nonlocal approximation coincides with the exact solution of (34) and (40). Moreover, if the excitation function is of low frequency only, i.e. $B_n = 0$ for all n for which $\frac{E_d}{E_0 L^2}(p_n)^2$ is of order one, then the two formulations will also provide similar results.

Elimination of high frequency excitation modes can be also accomplished by using a sufficiently coarse spatial discretization (or coarse finite element mesh) for numerical approximation of the nonlocal initial-boundary value problem.

Remark 2: It is appropriate to note that the nonlocal equation of motion (42) contains the information on the characteristic length. This can be seen by comparing the classical nonlocal continuum theory (see for example [18]) with the current model. Assuming constant weight function the spatial derivative of the nonlocal strain, $\bar{\varepsilon}$, [18] is given by:

$$\frac{d}{dx}\bar{\varepsilon} = \frac{1}{\chi}\int_{-\chi/2}^{\chi/2} u,_{xx}(x+s)ds = u,_{xx} + \frac{\chi^2}{24}u,_{xxxx} + \ldots \tag{49}$$

where χ is a characteristic size in the physical domain. Matching the coefficients of the fourth order term in (49) and (42) yields $E_d = \chi^2 E_0/24$. In the case of volume fraction α equal to *0.5* the relation between the characteristic size and the unit cell dimension is given as

$$\frac{\chi}{l} = \frac{\sqrt{2}\left|\frac{\rho_2 E_2}{\rho_1 E_1} - 1\right|}{\left(1 + \frac{\rho_2}{\rho_1}\right)\left(1 + \frac{E_2}{E_1}\right)} \tag{50}$$

An upper bound of this ratio (obtained by maximizing the ratio with respect to ρ_2/ρ_1 and E_2/E_1) is equal to $\sqrt{2}$. It can be easily shown that in the case of weight function given as $(\pi/2\chi)\cos(s\pi/\chi)$ the upper bound of the ratio χ/l is approximately 30% higher. For example, in concrete it has been observed [19] that the characteristic size is approximately three aggregates. Assuming that a typical volume fraction is approximately 0.5, the characteristic size approximately contains *1.5* unit cells. This agrees well with our model which predicts the characteristic size to be in the range of 1.4 to 1.8 unit cells depending on the choice of weight functions.

To this end we propose an alternative nonlocal approach by which the second order spatial derivative (42) is approximated by a second order temporal derivative by exploiting the following relation (for details see [20])

$$U_{,xx} = \frac{\rho_0}{E_0}\ddot{U} + O(\varepsilon^3) \tag{51}$$

which yields

$$\rho_0\ddot{U} - E_0 U_{,xx} - \rho_0 E_k \ddot{U}_{,xx} = 0 \tag{52}$$

where

$$E_k = \frac{E_d}{E_0} = \frac{[\alpha(1-\alpha)]^2(E_1\rho_1 - E_2\rho_2)^2\Omega^2}{12\rho_0^2[(1-\alpha)E_1 + \alpha E_2]^2} \tag{53}$$

Note that equation (52) is second-order in space, and thus two boundary conditions are sufficient. Since the highest spatial derivative appearing in this equation is second order the need for C^1 continuity is eliminated.

Equation (52) can be solved analytically for the aforementioned model problem by separation of variable, which yields:

$$U(x, t) = \sum_{n=1}^{\infty} B_n \sin\frac{p_n x}{L} \cos\left(\frac{p_n ct/L}{\sqrt{1 + \frac{E_d}{E_0 L^2}(p_n)^2}}\right) \tag{54}$$

It can be readily observed that solution (54) is well-behaved and convergent with increase of terms in the Fourier series. Comparison to the source problem in a heterogeneous medium will be conducted in Section 6.

5. Numerical Procedures

In this section, we focus on the finite element implementation of the “good” Boussinesq equation (52). Based on the usual weighted-residual approach, the weak statement of the problem is as follows: For $t \in (0, T_0]$, find $U(x, t) \in H_0^1(0, L)$, such that

$$\int_0^L \rho_0 A w \ddot{U} dx + \int_0^L E_0 A w_{,x} U_{,x} dx + \int_0^L \rho_0 E_k A w_{,x} \ddot{U}_{,x} dx =$$

$$E_0 A U_{,x} w(L) + \rho_0 E_k A \ddot{U}_{,x} w(L) \tag{55}$$

and

$$U(x, 0) = f(x) , \quad \dot{U}(x, 0) = g(x) \tag{56}$$

for all admissible test functions $w(x) \in H_0^1(0, L)$, where

$$H_0^1(0, L) = \{ w(x) \in H^1(0, L) \big| w(0) = 0 \} \tag{57}$$

$$H^1(0, L) = \{ q = q(x), x \in (0, L) | q, q_{,x} \in L^2(0, L) \} \tag{58}$$

with $L^2(0, L)$ denoting the set of square-integrable functions over $(0, L)$.

Introducing the finite element approximation into the above weak formulation leads to the semi-discrete equations of motion

$$\boldsymbol{M}\ddot{\boldsymbol{d}} + \boldsymbol{K}\boldsymbol{d} = \boldsymbol{F} \tag{59}$$

where $\boldsymbol{d}(t)$ is the vector of nodal values of displacements and $\boldsymbol{F}$ is the load vector; $\boldsymbol{M}$ and $\boldsymbol{K}$ are the mass and stiffness matrices, respectively:

$$\boldsymbol{M} = \sum_{e=1}^{Ne} \boldsymbol{m}^{\boldsymbol{e}}, \qquad \boldsymbol{K} = \sum_{e=1}^{Ne} \boldsymbol{k}^{\boldsymbol{e}} \tag{60}$$

$$\boldsymbol{m}^{\boldsymbol{e}} = \int_{L_e} \rho_0 A \boldsymbol{N}^{\boldsymbol{T}} \boldsymbol{N} dx + \int_{L_e} \rho_0 E_k A \boldsymbol{N}^{\boldsymbol{T}}_{,x} \boldsymbol{N}_{,x} dx, \qquad \boldsymbol{k}^{\boldsymbol{e}} = \int_{L_e} E_0 A \boldsymbol{N}^{\boldsymbol{T}}_{,x} \boldsymbol{N}_{,x} dx \tag{61}$$

$$\boldsymbol{F} = \left\{ q(t) + \frac{\rho_0 E_k}{E_0} \ddot{q}(t) \right\}_{x = L} \tag{62}$$

where $\boldsymbol{m}^{\boldsymbol{e}}$, $\boldsymbol{k}^{\boldsymbol{e}}$ and $\boldsymbol{N}$ are element mass matrix, stiffness matrix and shape function, respectively.

Equation (59) can be integrated in the time domain by using standard time integration schemes.

<u>*Remark 3:*</u> For (62) to be valid the load $q(t)$ must be twice differentiable in time or approximated as such. Based on (35) it can be easily shown that

$$\frac{\rho_0 E_k}{E_0} \le \frac{\bar{T}^2}{12} \tag{63}$$

where $\bar{T}$ is the time required for the wave to travel through the unit cell. In other words, for the second term in (62) to be comparable in magnitude to the first term the load period should be $\pi\bar{T}/\sqrt{12}$. In the present manuscript attention is restricted to load frequencies which are significantly larger than $\bar{T}$ and thus the second term in (62) is neglected.

6. Numerical Results and Discussion

To validate the proposed nonlocal model, we consider two problems with different loading cases. For each problem, a reference solution of the source problem for heterogeneous solid is constructed by utilizing a fine mesh with element size comparable to the size of the microconstituents.

Problem 1: Macro-domain $L = 40$ *m;* unit cell $l = 0.2$ *m* composed of two material constituents with $E_1 = 120$ *GPa,* $E_2 = 6$ *GPa,* $\rho_1 = 8000$ *Kg/m*^{3}, $\rho_2 = 3000$ *Kg/m*^{3};

volume fraction $\alpha = 0.5$. At $x = 20\ m$ an initial disturbance $f(x)$ in displacement field

$$f(x) = f_0 a_0 [x-(x_0-\delta)]^2 [x-(x_0+\delta)]^2 \{1-h[x-(x_0+\delta)]\} \cdot \{1-h(x_0-\delta-x)\}$$

is applied; $a_0 = 1/\delta^4$ and $h(x)$ denote the Heaviside step function; f_0, x_0 and δ are the magnitude, the location of the maximum value and the half width of the initial pulse, respectively. The pulse is similar in shape to the Gaussian distribution function.

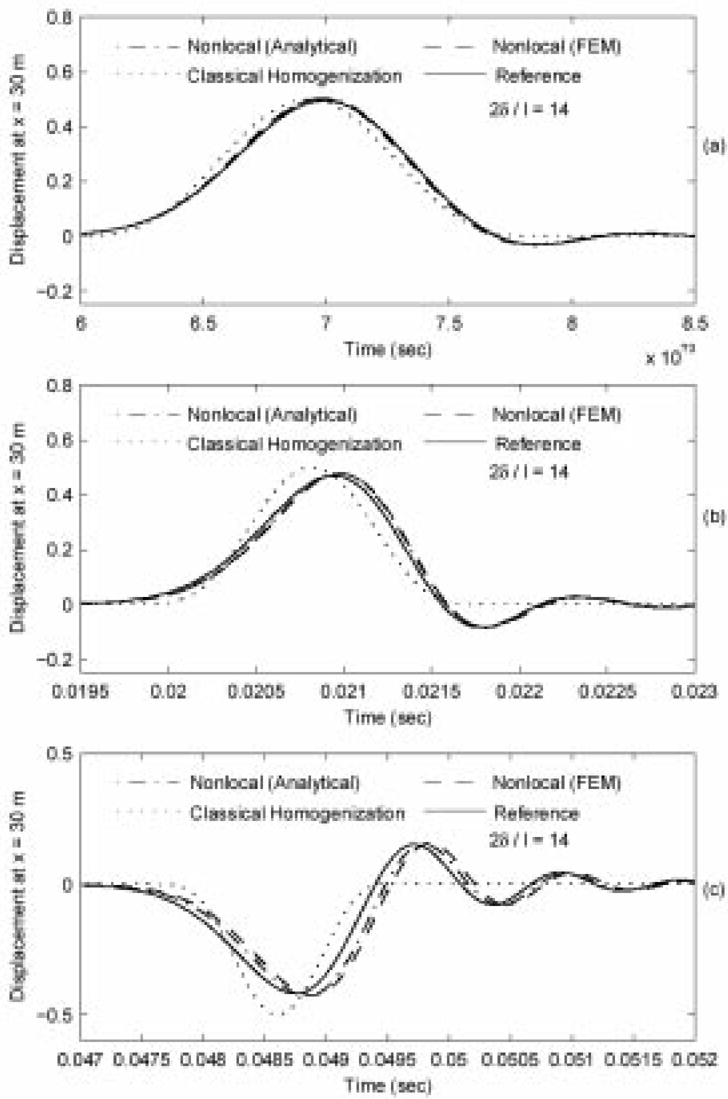

Figure 2: The response with an initial disturbance in displacement ($\delta = 1.4m$).

The calculated homogenized material properties are: $E_0 = 11.43\ GPa$, $\rho_0 = 5500\ Kg/m^3$ and $E_d = 1.76 \times 10^7\ N$. In this case, $E_1/E_2 = 20$ and the ratio of impedance of the two material constituents is $r = 7.30$. The magnitude of the initial pulse is $f_0 = 1.0\ m$.

We plot the time-varying displacement at $x = 30\ m$ in Figures 2 and 3, for the cases of $\delta = 1.4\ m$, and $\delta = 0.6\ m$, respectively. The corresponding ratios between the pulse width and the unit cell dimension $2\delta/l$ are 14 and 6, respectively. In each of the figures, we show three time windows and compare the reference solution of the heterogeneous solid, the finite element solution predicted by the classical homogenization U_0, and the analytical and the finite element solutions of the "good" Boussinesq problem.

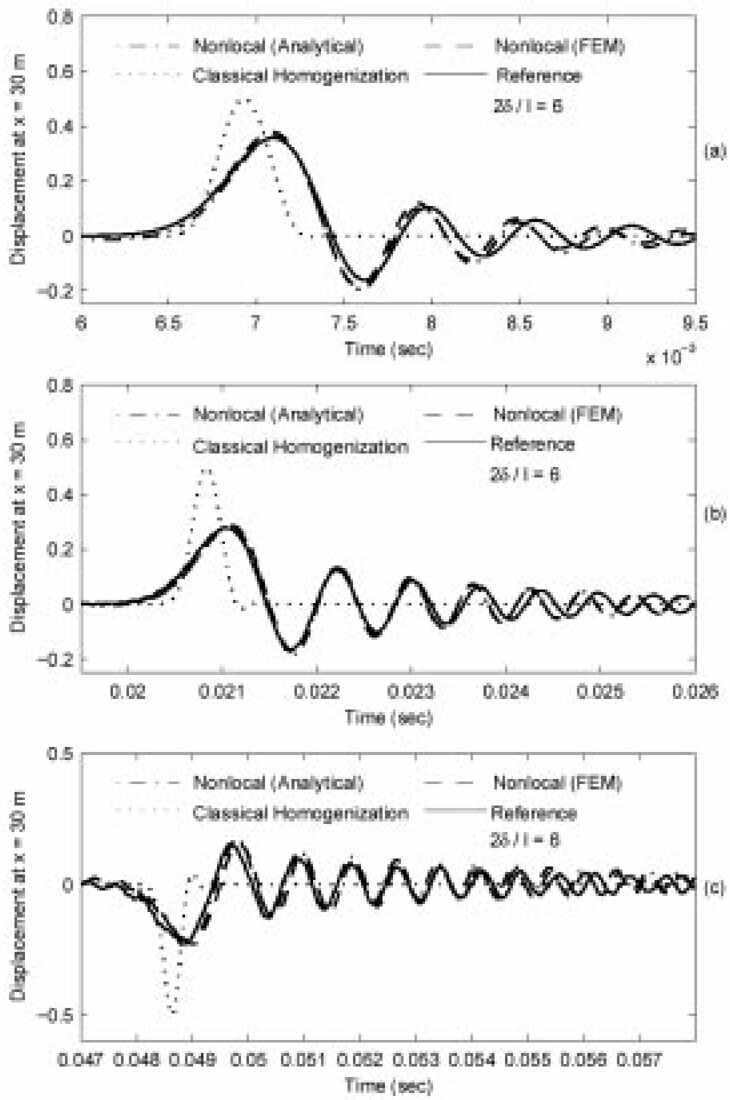

Figure 3: The domain with an initial disturbance in displacement ($\delta = 0.6m$)

Problem 2: The size of the domain and that of the unit cell are $L = 1$ *m* and $l = 0.02$ *m*, respectively. The material properties of the two constituents are $E_1 = 200$ *GPa*, $E_2 = 5$ *GPa*, $\rho_1 = \rho_2 = 8000$ *Kg/m*^{3}, and $\alpha = 0.5$. The calculated homogenized material properties are: $E_0 = 9.76$ *GPa*, $\rho_0 = 8000$ *Kg/m*^{3} and $E_d = 7.36 \times 10^4$ *N*. In this case, $E_1/E_2 = 40$.

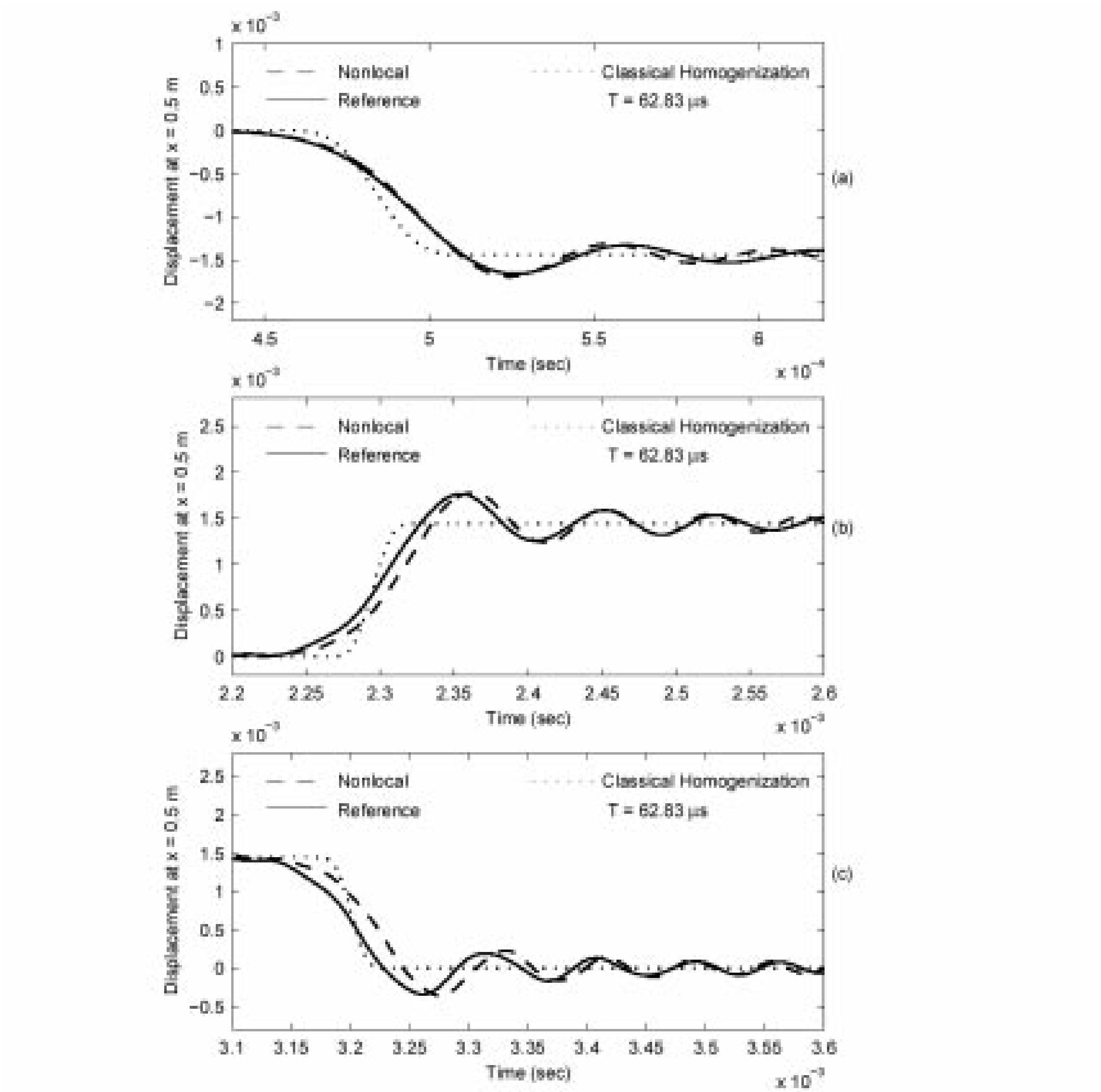

Figure 4: The response with an impact load (pulse duration $T = 62.83\mu s$).

The bar is subjected to an impact load $q(t) = q_0 a_0 t^4 (t-T)^4 [1 - h(t-T)]$ at $l = 1$ *m*, where T is the duration of the impact pulse, $q_0 = -50$ *KN* and a_0 is scaled in such a way that $0 \le q(t) \le q_0$. The time-varying displacements at $x = 0.5$ *m* are plotted in Figures 5 and 6, which correspond to pulse duration $T = 62.83\mu s$ and $T = 15.71\mu s$, respectively. In each of the two figures, there are three responses corresponding to the reference solution, the finite element solution predicted by the classical homogenization U_0 and the finite element solution of the “good” Boussinesq equation.

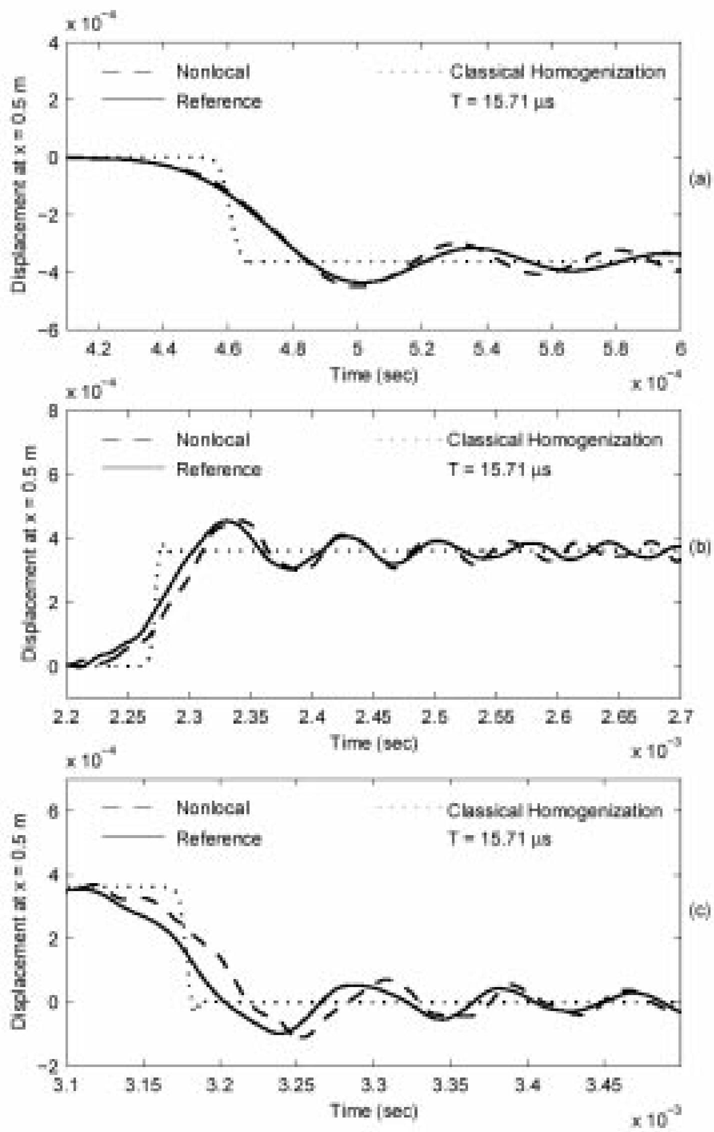

Figure 5: The domain with an impact load (pulse duration $T = 15.71\mu s$).

The phenomenon of dispersion can be clearly observed in Figures 2-5. When the width of the initial disturbance in displacement is much larger than the unit cell size or the impact pulse duration is comparatively long, which corresponds to the cases in Figure 2 and Figure 4, the pulse almost maintains its initial shape except for some small wiggles at the wavefront. In this case, the classical (leading-order) homogenization provides a crude approximation to the response of the heterogeneous solid. However, when the pulse width of the initial disturbance is comparable to the dimension of the unit cell or the impact pulse duration is very short, which are the cases in Figure 3 and Figure 5, the wave becomes strongly dispersive and the classical homogenization errs badly. On the other hand, the nonlocal dispersive model proposed in this paper provides a good approximation to the response of heterogeneous solid.

Acknowledgment

This work was supported by the Sandia National Laboratories under Contract DE-AL04-94AL8500, the Office of Naval Research through grant number N00014-97-1-0687, and the Japan Society for the Promotion of Science under contract number Heisei 11-nendo 06542.

References

1 Sanchez-Palencia, E., “Non-homogeneous Media and Vibration Theory”, Springer, Berlin, 1980

2 Benssousan, A., Lions, J.L. and Papanicoulau, G., “Asymptotic Analysis for Periodic Structures”, North Holland, Amsterdam, 1978.

3 Bakhvalov, N.S., and Panasenko, G.P., “Homogenization: Averaging Processes in Periodic Media”, Kluwer, Dordrecht, 1989.

4 Gambin, B., and Kroner, E., “High order terms in the homogenized stress-strain relation of periodic elastic media”, Phys. Stat. Sol., Vol.51, 1989, pp. 513-519.

5 Boutin, C., “Microstructural effects in elastic composites”, Int. J. Solids Struct. 33(7), 1996, pp.1023-1051.

6 Boutin, C., and Auriault, J.L, “Rayleigh scattering in elastic composite materials”, Int. J. Engng. Sci. 31(12), 1993, pp.1669-1689

7 Kevorkian, J., and Bosley, D.L., “Multiple-scale homogenization for weakly nonlinear conservation laws with rapid spatial fluctuations:, Studies in Applied Mathematics, Vol.101, 1998, pp.127-183.

8 Fish, J., and Chen, W., “High-order homogenization of initial/boundary-value problems”, accepted by ASCE Journal of Engineering Mechanics, 2000.

9 Chen, W., and Fish, J., “A dispersive model for wave propagation in periodic heterogeneous media based on homogenization with multiple spatial and temporal scales”, accepted by ASME Journal of Applied Mechanics, 2000.

10 Santosa, F., and Symes. W.W., “A dispersive effective medium for wave propagation in periodic composites”, SIAM J. Appl. Math., 51(4), 1991, pp. 984-1005.

11 Francfort, G.A., “Homogenization and linear thermoelasticity”, SIAM J. Math. Anal., 14(4), 1983, pp. 696-708.

12 Mei, C.C., Auriault J.L., and Ng, C.O., “Some applications of the homogenization

theory”, in: Advances in Applied Mechanics, Vol. 32, Hutchinson, J.W., and Wu, T.Y., eds., Academic Press, Boston, 1996, pp. 277-348.

13 Boutin, C., and Auriault, J.L., “Dynamic behavior of porous media saturated by a viscoelastic fluid. Application to bituminous concretes”, Int. J. Engng. Sci., 28(11), 1990, pp.1157-1181.

14 Carey, G.F., and Oden, J.T., “Finite Elements, A Second Course”, Vol. II, Prentice-Hall, New Jersey, 1983.

15 Carey, G.F., and Oden, J.T., “Finite Elements, Mathematical Aspects”, Vol. IV, Prentice-Hall, New Jersey, 1983.

16 Maugin, G.A., “Physical and mathematical models of nonlinear waves in solids”, in: Nonlinear Waves in Solids, Jeffrey, A., and Engelbrecht, J., eds., Springer, Wien-New York, 1994.

17 Whitham, G.B., “Linear and Nonlinear Waves”, John Wiley & Sons, New York, 1974.

18 Z. Bazant, T.B.Belytschko and T.P.Chang, “Continuum theory for strain-softening,” Journal of Engineering Mechanics, Vol. 110, No.12, pp.1666-1692, 1984.

19 G. Pijaudier-Cabot and Z.P. Bazant, “Nonlocal damage theory,” Journal of Engineering Mechanics, Vol. 113, No.10, pp.1512-1533, 1987.

20 J. Fish, W. Chen and G. Nagai, “Nonlocal Dispersive Model For Wave Propagation In Heterogeneous Media. Part 2: Multi-Dimensional Case,” International Journal for Numerical Methods in Engineering, 2001.